

Dariusz **ZACZYK**
Marcin **FICE**

ELECTRIC POWER DISTRIBUTION SYSTEM IN A HYBRID VEHICLE

Abstract. The paper presents problems associated with proper design of an electrical system of a vehicle with a hybrid propulsion system (internal combustion + electric). Topology of the system is shown along with results obtained: tables of parameters of a high current electrical system of a hybrid vehicle. The paper describes major components of the design work, including power balance, safeguards, wire cross sections, determination of the working point of a fan and soft start system for the electric motor. In conclusion, reference is made to the practical application of the calculation results.

Keywords: hybrid vehicle, series hybrid drive, power distribution, electric motor with permanent magnets

1. INTRODUCTION

In a number of research works related to drives for land vehicles (cars, special purpose vehicles, military vehicles, etc.), both here and abroad, solutions are sought that would enable taking the most advantage of energy sources: electrical or internal combustion propulsion. Among the many solutions applied in practice there is a rising popularity of vehicles with hybrid drives [1], [2], [3]: internal combustion engine and electric motor. In a project [4] being implemented and entitled "Multitask, engineering vehicle with hybrid drive" (WIPH), a hybrid drive was also used. The adopted solution included a series hybrid system.

The vehicle's drive system used two electric motors with 70 kW continuous rating and 120 kW maximum rating each. The motors were of the PMSM type (synchronous motors with permanent magnets) which feature high efficiency and very favourable power to weight ratio. The use of high output drives of reduced dimensions in the vehicle was necessary to meet the adopted requirement of maximum total weight of 6000 kg and to attain the best possible traction characteristics.

The vehicle's traction system uses metal+rubber tracks (polymer tracks to be the final design) driven by electric motors, planetary gears with sprocket wheels. For safety reasons the planetary gears are fitted with a hydraulic passive safety brake. The main power source is a EURO 5 internal combustion engine providing 150 kW output at 3000 rpm. This engine drives an electric generator with a continuous output of 150 kW and maximum output of 225 kW. The generator charges a battery pack through an inverter. The batteries are a power source for the electric propulsion motors.

One of the main requirements of the project is that the vehicle should operate in two configurations:

- remotely controlled self-contained chassis;
- chassis with a cab with controls.

Fig. 1 presents a virtual design of a hybrid vehicle.



Fig. 1. Engineering vehicle with hybrid drive

Those interested may find WIPH vehicle design described in more detail in [5]. One of the major issues in the work conducted [4] is the proper design of the power distribution system which must take into account extremely adverse operating conditions. And this is the principal theme of this paper.

2. STRUCTURE OF THE POWER DISTRIBUTION SYSTEM OF THE VEHICLE UNDER DESIGN

The powertrain of the vehicle includes a hybrid internal combustion+electric system in a series arrangement shown in Fig. 2. The power system outputs are connected in parallel to two inverters responsible for powering the electric propulsion motors. The propulsion motors operate in the generator mode during regenerative braking of the vehicle and when turning the vehicle by moving the tracks in opposite directions (vehicle spins around its centre). The surplus energy recovered during braking or when the vehicle is not moving is transferred from the electric generator via the power distribution system (PDS) to a battery pack.

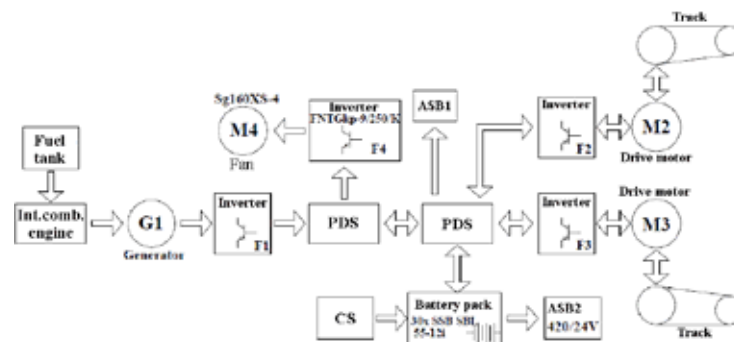


Fig. 2. Block diagram of a multitask engineering vehicle with a hybrid drive (authors' study)

The battery pack comprises lead-acid cells SSB SBL 55-12i. The capacity of the battery pack is 55 Ah and is a compromise between weight and maximum discharge current attainable in the mode of exclusively electrical operation. The energy losses during the

operation of the drive system cause heating of the system components. Excessive temperature rise could damage them. Temperature is maintained at a permissible level by the central cooling system. The latter is an active system where air is forced through a radiator filled with a cooling medium. Air flow is induced by a fan driven by a three-phase squirrel-cage induction motor powered via an inverter. The power distribution system is additionally provided with a parking charging system (CS) for use with a 230V single-phase mains and auxiliaries switchboards (ASB1) and (ASB2).

3. POWER BALANCE IN THE DRIVE SYSTEM

When designing the electric system special attention was paid to the maximum output of the propulsion motors in order to meet the adopted requirements of the vehicle travel cycles. It was important to determine the values of supply voltages for the individual components of the electric circuit to ensure that the maximum permissible supply voltage in the electric system falls within the range of permissible voltages for all devices in the system and at the same time the maximum current in the battery circuit. In this case the maximum system voltage of 410V DC was adopted.

In order to properly design the electric system by sizing wire cross sections, accessory equipment and protection equipment, a detailed analysis of the system was carried out and the circuit current values were determined for various operating conditions. The power balance was determined for drive system operation under rated conditions, maximum output and in the mode of exclusively electrical operation. The current protection fuse link ratings and wire cross sections were determined on the basis of above. Additionally, voltage drops in the system were determined and compared to values specified in standard PN-S-76021, which confirmed the correctness of wire cross section sizing.

For the purpose of power balance determination, a simplified block diagram of the system was drawn (Fig. 3), where designations of the individual circuits listed in tables (1), (2) and (3) were placed. Detailed calculations are provided in the bachelor's thesis [6].

The voltages adopted for calculating currents in the individual DC circuits were 410 V for hybrid operation and 300 V for exclusively electrical operation.

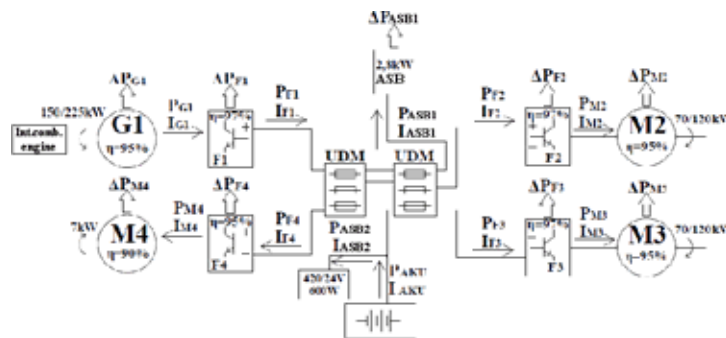


Fig. 3. Power balance diagram with system parameters shown (P - output, I - current, η - efficiencies)

4. PROTECTION SIZING

The project under way, technology demonstrator, will undergo a lot of research and testing. To ensure as far as possible trouble-free and user-friendly operation, a number of protection devices were installed in the high-voltage electrical system.

The table lists rated (N), maximum (MAX) and electrical operation mode (ELE) values for selected current paths (designated with indices in Fig. 3) in the vehicle.

Table 1. Protection sizing for vehicle circuits

Current path	P_N [kW]	I_N [A]	P_{MAX} [kW]	I_{MAX} [A]	P_{ELE} [kW]	I_{ELE} [A]	Protection device	Trip value
$P_{G1}; I_{G1}$	86	131	143	219	0	0	-	-
$P_{F1}; I_{F1}$	83	202	139	337	0	0	FWH-200B	$t_{I_{MAX}} \geq 200s$
$P_{M4}; I_{M4}$	7.8	19	7.8	19	0	0	-	-
$P_{F4}; I_{F4}$	8.2	20	8.2	20	5	19	FWH-35B	Short-circuit
$P_{M2}; I_{M2}$	74	113	126	194	25.3	39	-	-
$P_{F2}; I_{F2}$	76	185	130	317	26	87	FWH-200B	$t_{I_{MAX}} \geq 200s$
$P_{M3}; I_{M3}$	74	113	126	194	25.3	39	-	-
$P_{F3}; I_{F3}$	76	185	130	317	26	87	FWH-200B	$t_{I_{MAX}} \geq 200s$
$P_{Aku}; I_{Aku}$	81	197	135	328	57	191	NH-SI 3 160A GG AC690V AK	$t_{I_{MAX}} \geq 130s$
$P_{ASB1}; I_{ASB1}$	2.9	7.1	3.65	8.9	0	0	DCM 8A/600Vdc	Short-circuit
$P_{ASB2}; I_{ASB2}$	0.6	1.46	0.6	1.46	0	0	Z-SLS-B 2A	Short-circuit

All protection devices were sized on the basis of time-current characteristics of the fuse links [7], [8], [9]. The sized protection devices withstand rated current value for S1 operation.

5. WIRE CROSS SECTION SIZING

Equally important in designing an electric system is the proper sizing of cross sections of wires used in the system. The wires should have been sized in such way that the following condition had to be satisfied for a long duration current:

$$I_N < K_P * I_{DD}$$

where: I_N - Design long duration current,

K_P - Correction factor dependent on wire arrangement (0.70 for three conductors; 0.80 for two conductors, with allowance for the adverse effect of increased temperature),

I_{DD} - Long duration current capacity specified by manufacturer.

Table 2 lists wire cross sections sized for continuous operation and short time overload (max. 20 s) with maximum power. Due to the large currents flowing in the circuits of the propulsion system and the use of power electronic converters and due to the short distance between control systems and low-voltage equipment, the requirements of the electromagnetic compatibility (EMC) were also taken into consideration when sizing high-current wires. For this reason shielded wires RADOX 4 GKW-AX 1800V MM S, EMC [10] were used in the system.

Table 2. Wire cross section sizing

Current path	I_N [A]	I_{MAX} [A]	P_P [mm ²]	$K_P * I_{DD}$	$I_N < K_P * I_{DD}$	$I_{MAX} < K_P * I_{DD}$
G1 - F1	131	219	50	$0.70 * 359A = 251A$	$131A < 251A$	$219A < 251A$
F1 - PDS	202	337	50	$0.80 * 359A = 287A$	$202A < 287A$	$337A < 287A$
M4 - F4	19	19	4	$0.70 * 67A = 47A$	$19A < 47A$	$19A < 47A$
F4 - PDS	20	20	4	$0.80 * 67A = 54A$	$20A < 54A$	$20A < 54A$
M2 - F2	113	194	35	$0.70 * 285A = 200A$	$113A < 200A$	$194A < 200A$
F2 - PDS	185	317	50	$0.80 * 359A = 287A$	$185A < 287A$	$317A < 287A$
M3 - F3	113	194	35	$0.70 * 285A = 200A$	$113A < 200A$	$194A < 200A$
F3 - PDS	185	317	50	$0.80 * 359A = 287A$	$185A < 287A$	$317A < 287A$
Aku - PDS	197	328	50	$0.80 * 359A = 287A$	$197A < 287A$	$328A < 287A$
ASB1-PDS	7.1	8.9	1.5	$0.80 * 36 = 23.2A$	$7.1A < 23.2A$	$8.9A < 23.2A$
ASB2 420/24V -Aku	1.46	1.46	1.5	$0.80 * 36 = 28.8A$	$1.46A < 28.8A$	$1.46A < 28.8A$

6. DETERMINATION OF VOLTAGE DROPS ALONG WIRE

Another criterion of proper sizing of wire cross sections is the determination of voltage drops along the wires. The higher the voltage drop, the larger are the power losses in the system. Voltage drop is defined as the percentage of voltage across the wire in relation to the voltage rating of the system. There are no standards or guidelines for voltage drops in electric systems of electric and hybrid vehicles. For this reason the PN-S-76021 standard [14] was applied (according to the standard the maximum voltage drop in the battery circuit is 3.5%, and in other circuits – 10%). Table 3 lists voltage drops for the rated and maximum values of load current.

Table 3. Voltage drops in the individual circuits of the electric system of the vehicle

Current path	L [m]	U_N	$\Delta U\%$ for I_N	$\Delta U\%$ for I_{max}
$P_{G1}; I_{G1}$	6	3-f 400V AC $\cos\phi = 0.94$	0.11%	0.18%
$P_{F1}; I_{F1}$	8	410 VDC	0.27%	0.45%
$P_{M4}; I_{M4}$	9	289 V 3-f AC $\cos\phi = 0.81$	0.35%	0.35%
$P_{F4}; I_{F4}$	6	410 VDC	0.25%	0.25%
$P_{M2}; I_{M2}$	3	3-f 400V AC $\cos\phi = 0.94$	0.067%	0.11%
$P_{F2}; I_{F2}$	6	410 VDC	0.19%	0.32%
$P_{M3}; I_{M3}$	3	3-f 400V AC $\cos\phi = 0.94$	0.067%	0.11%
$P_{F3}; I_{F3}$	6	410 VDC	0.19%	0.32%

$P_{Aku}; I_{Aku}$	8	410 VDC	0.26%	0.44%
$P_{BSC}; I_{BSC}$	6	410 VDC	0.23%	0.29%
$P_{Sup}; I_{Sup}$	6	410 VDC	0.05%	0.05%

Voltage drops listed in Table 3 were calculated using the following formulae:

- voltage drops in direct current circuits: [11]

$$\Delta U\% = \frac{2 * I * L * 100}{\sigma * U_N * s}$$

- voltage drops in 3-phase alternating current circuits: [11]

$$\Delta U\% = \frac{\sqrt{3} * I * L * \cos\varphi * 100}{\sigma * U * s}$$

where: $\Delta U\%$ - percentage voltage drop along wire ,

σ - conductivity of copper wire. The adopted value is $58 \frac{m}{\Omega * mm^2}$,
 U - rated voltage in the system,
 I - current in the circuit,
 L - wire length,
 $\cos\varphi$ - power factor,
 s - wire cross section.

7. DETERMINATION OF THE WORKING POINT OF THE MAIN FAN MOTOR

Ensuring the set operating temperature ranges depends largely on the choice of the working point of the motor driving the fan impeller creating the required cooling air flow. The fan in the cooling system is driven by a squirrel-cage induction motor (SG160XS-4) fabricated by the KOMEL Institute for this specific application. The rated motor supply voltage is 3x400 VAC, rated speed 4000 rpm (at supply frequency of 137 Hz), rated current is 35.6A, and the power rating is 18kW. Figure 4 presents the performance characteristics of the motor used across the entire speed range and the characteristics of the fan.

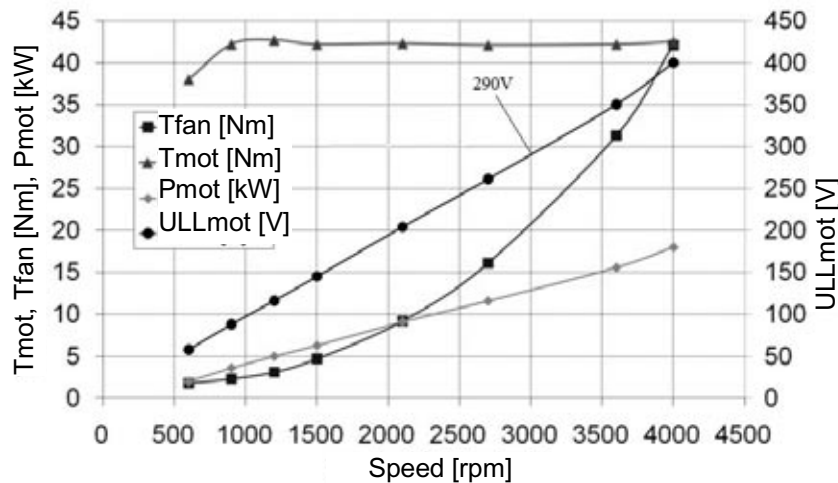


Fig. 4. Graph representing the motor performance when controlled under constant U/f ratio [12]

The on-board voltage in the vehicle under design is 420V DC. For this reason an inverter had to be used with a DC input and wide operating voltage range (300 – 420V DC). The inverter used (FNTGkp-9/500/V) was designed specifically for the cooling system by ENEL [15].

The RMS value of the phase-to-phase voltage of the inverter is:

$$U_{rms} = \frac{410}{\sqrt{2}} = 289,9 \text{ V}$$

where: U_{rms} - phase-to-phase voltage.

The calculated supply voltage of the fan motor is 3x290VAC. This means reduced speed of the motor. When motor supply voltage is decreased under scalar control, a constant ratio of supply voltage to frequency should be maintained.

$$\frac{U}{f} = \frac{400}{137} = 2,92$$

where: U/f- voltage to frequency ratio. The frequency for the set supply voltage in the vehicle is 99.3 Hz.

The speed of the motor driving the cooling system fan under scalar control and voltage of 290 V, as read from Fig. 4, is ca. 3000 rpm. The maximum torque generated by the motor is 42 Nm, whereas the torque of the fan running at 3000 rpm is 22 Nm. Upon calculating the load torque into power:

$$P = M * \frac{2 * \pi * n}{60}$$

the load of the cooling system fan on the motor at 3000 rpm is ca. 7 kW. Therefore there is a considerable driving torque margin of the motor. The motor output adopted for calculating the power balance was 7 kW.

In order to verify proper operation of the inverter-fan system, current was measured as a function of the frequency generated by the inverter. The measured characteristic is shown in Fig. 5. At 110 Hz the motor current rating is about 35 A.

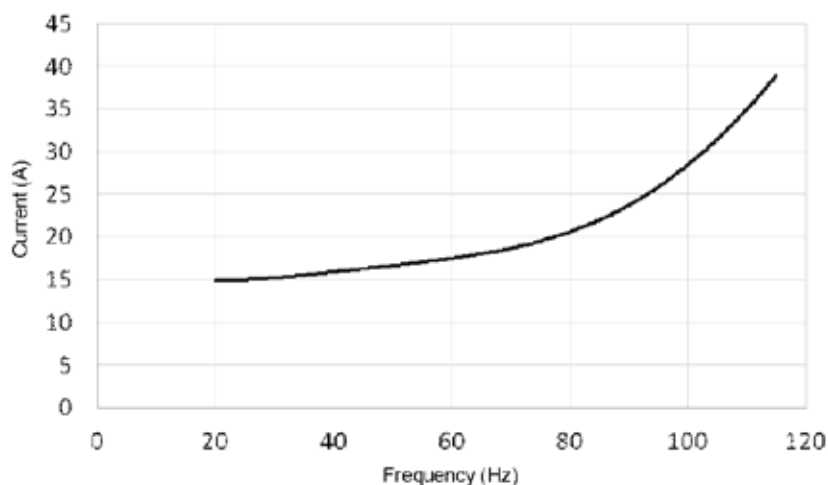


Fig. 5. Motor current vs. supply voltage frequency of the main fan motor SG 160XS-4

8. SOFT START SYSTEM

Electric motors of the vehicle drive system are powered by modern power electronic converters. These inverters have large capacitances at supply input, the values of which are given in specification sheets. When full voltage is applied, the flowing current is defined by the relationship:

$$i_c(t) = C \frac{du_c(t)}{dt}$$

where: $du_c(t)$ - voltage rise on capacitor,
 dt - time during which voltage rise occurred.

The occurrence of such currents might affect the switch contacts during commutation and cause contact burning and eventually failure of the supply line. In order to limit the starting current of the inverters, a simple soft start system was applied. Such a system may be set up using a resistor of adequate power rating connected in series into the circuit of voltage source and inverters. The soft start system used in the vehicle will consist of a power resistor allowing the limitation of the maximum starting current to about 20 A, and of semiconductor contactors that will allow for the complete elimination of switching surges, as in that case no commutation occurs.

The resistor rating was calculated using the Ohm's law:

$$R = \frac{U}{I} = \frac{410}{20} = 20,5 \Omega$$

where: R - resistor resistance,
 U_N - system voltage rating,
 I - permissible current in the circuit.

The calculated required resistance is 20.5 Ω . A 20 Ω resistor was eventually used. The maximum current in the soft start circuit was determined:

$$I = \frac{U}{R} = \frac{410}{20} = 10,5 A$$

In order to verify calculation results and estimate the power dissipated in the resistors, a simulation of the inverter charging current, voltage of the source and voltage on the inverters was conducted. This simulation was carried out by means of Matlab Simulink [16] using a wiring diagram shown in Fig 6. The system comprises a constant voltage source 410V (BAT), two semiconductor contactors CRYDOM - SSC800-25-12 – SSR (K1 and K2), two soft start resistors, three inverters of the drive system, one inverter FNT Gkp-9/500/V of the cooling system, ASB converter. Fig. 7 shows voltage curves for all capacitances and current curve, and Fig. 8 shows the power dissipated on the soft start system resistors.

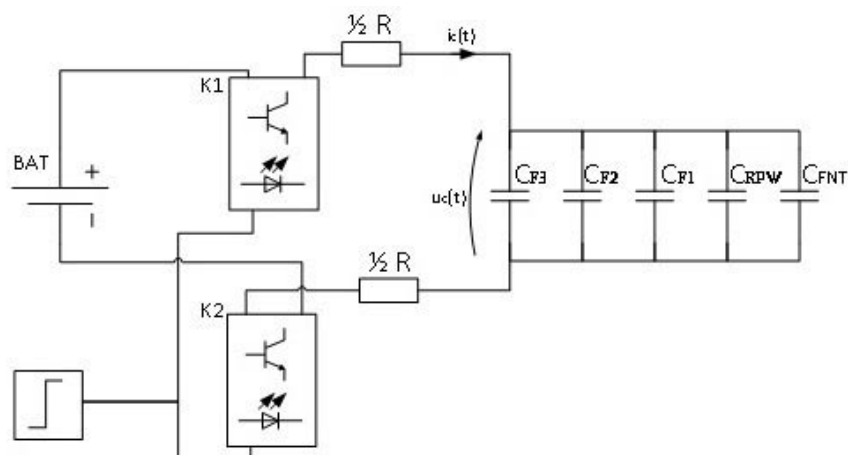


Fig. 6. Model of the soft start system

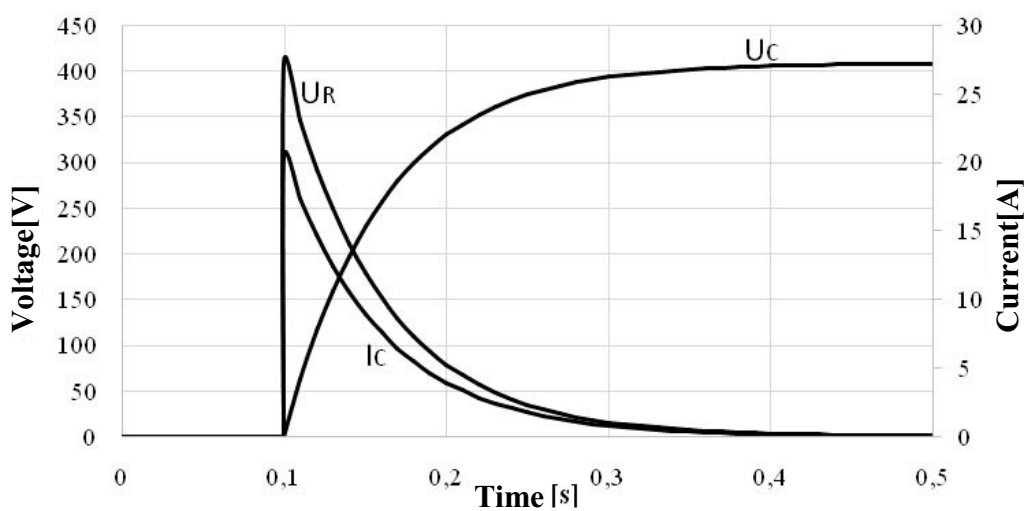


Fig. 7. Curves of voltages across resistors and capacitors and of currents in the resistors of the soft start circuit

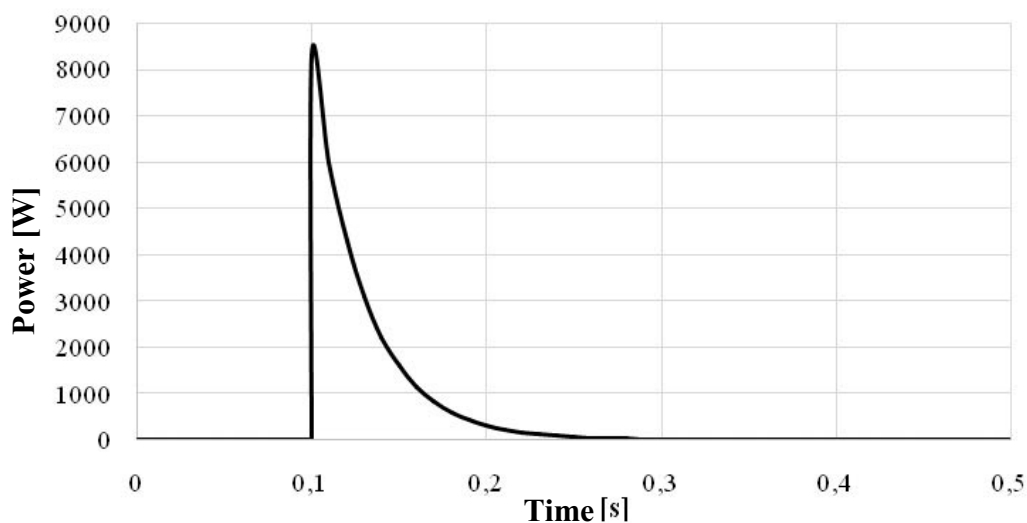


Fig. 8. Curves of power dissipated on resistors of the soft start circuit

The maximum power attained in the system is ca. 8.2 kW, the energy dissipated on resistors is ca. 3 kJ. The resistor power rating was sized to avoid failure caused by overheating.

$$P = I^2 \cdot R$$

Two resistors: $R=10 \Omega$ $P=600 \text{ W}$ connected in series provide $R=20 \Omega$ and $P=1200 \text{ W}$. This means that there will be a 7-fold overload on the resistor and according to Fig. 9 the resistor will operate for about 4 secs.

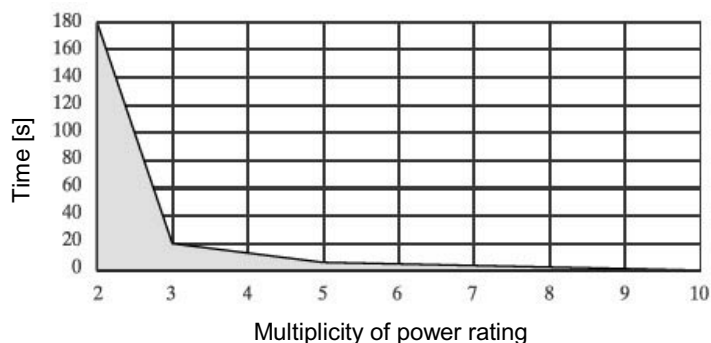


Fig. 9. Example of a resistor overload characteristic [13]

Royal Ohm HEWRB0J0100600 limiting resistors were selected.

9. SUMMARY

The calculations, simulations and power balances were the basis for the practical implementation of the WIPH project technical documentation, which in the next phase is applied in technology demonstrator. Power balances were drawn up for various operating modes of the system. The currents in the individual circuits of the system were determined. These were important data that helped select power cables of appropriate specifications to enable correct, trouble-free and, above all, safe operation of the entire system.

As in the vehicle, in addition to high-current circuits, there are also low-voltage control systems, the EMC requirements were also taken into account in the selection of conductors. For this reason screened wires were used in the drive system.

The working point of the induction motor driving the fan was determined, which showed that when using the selected fan, there was a considerable driving torque margin of the motor. Therefore, if there is need to use a larger fan, the need to modify the drive system is avoided. In addition, control parameters of the squirrel cage induction motor were determined, which may enable, if necessary, lower its output in the case of reduced demand for the power of the cooling system.

A soft start module was devised to avoid commutation surges when starting the electric circuit. Resistors of the soft start system were sized by making calculations. A system simulation was run to verify the correctness of calculations.

Determined voltage drops on high-current wires show that standards for vehicle electrical systems are met. As there are no standards or guidelines for voltage drops in electric systems of electric vehicles, the PN-S-76021 [14] standard was applied. This standard applies to electric systems in automotive vehicles.

The WIPH vehicle is equipped with modern electrical components having a number of integral protection devices and temperature sensors for monitoring the operation of the system, which has a beneficial effect on the safety and reliability of the vehicle.

The project [4], in its final stage, calls for carrying out factory acceptance tests and traction tests of the technology demonstrator. These will verify the theoretical studies (analyses, calculations, simulations) on a physical object - technology demonstrator - under real-world operating conditions (open terrain).

10. REFERENCES

- [1] Szumanowski A.: Pojazdy ekologiczne - przyszłość samochodów hybrydowych. <http://www.iinte.edu.pl/PM75/sesja4.pdf>, [Retrieved on: 5 May 2015].
- [2] <http://www.toyota.pl/hybrid-innovation/index.json>, [Retrieved on: 5 May 2015].
- [3] http://militarium.net/index-phppoptioncom_contentviewarticleid79polskie-autonomiczne-podwozie-gsienicowe-z-napdem-hybrydowymcatid7polskie-projektyitemid9/, [Retrieved on: 5 May 2015].
http://www.kms.polsl.pl/zastosowanie_badan_w_praktyce.php?p=zb1, [Retrieved on: 5 May 2015].
<http://www.militaryrok.pl/index.php/pojazdy-gsienicowe/954-autonomiczna-i-hybrydowa.html>, [Retrieved on: 10 May 2015].
- [4] Wielozadaniowy, inżynieryjny pojazd z napędem hybrydowym. I Konkurs Programu Badań Stosowanych. Umowa nr PBS1/A6/15/2013. NCBIR. Warszawa, January 2013.
- [5] Mężyk A., Klein W., Czapła T., Skowron K., Grabania M.Ł.: Pojazd gąsienicowy z napędem hybrydowym. Szybkobieżne Pojazdy Gąsienicowe (38), No. 3/2015 (pp. 81-94) OBRUM sp. z o.o. Gliwice, September 2015.
- [6] Zaczyk D.: „Projekt instalacji elektrycznej pojazdu hybrydowego”. Bachelor’s Thesis supervised by Dr Marcina Fice. Faculty of Electrical Engineering. Silesian University of Technology. Gliwice 2014.
- [7] http://cooper-bussmann.com/products/North-American-High-Speed-fuses/FWH-500V-North-American-High-Speed-Fuse_94.html#.VADjMWO4Gtc, [Retrieved on: 8 August 2014].
- [8] http://www.efen.com.pl/efen/katalogi/01_N.pdf, [Retrieved on: 8 August 2014].
- [9] http://www.cooperindustries.com/content/dam/public/bussmann/Electrical/Resources/product-datasheets-a/Bus_Ele_DS_2038_DCM.pdf, [Retrieved on: 8 August 2014].
- [10] <http://www.aste.pl/>, [Retrieved on: 8 August 2014].
- [11] <http://www.prs.pl/dzialalnosc-badawczo-rozwojowa/programy-obliczeniowe.html>, [Retrieved on: 8 August 2014].
- [12] Pistelok P., Czaja T.: Silnik klatkowy jako napęd wentylatora w trudnych warunkach pracy. Branżowy Ośrodek Badawczo-Rozwojowy Maszyn Elektrycznych KOMEL. Katowice 2011.
- [13] DACPOL Sp. z o. o. Catalogue, Issue 16.
- [14] PN-S-76021:1998/Az1:2001. Instalacja elektryczna pojazdów samochodowych. Wymagania i metody badań.
- [15] http://www.enel-automatyka.pl/o_firmie.htm, [Retrieved on: 8 August 2014].
- [16] <http://www.mathworks.com/products/simulink/>, [Retrieved on: 5 May 2015].

Results of the project titled "Multitask engineering vehicle with hybrid drive" financed by NCBiR (National Centre for Research and Development), as part of 1st Applied Studies Programme (contract no. PBS1/A6/15/2013), are referred to in this paper.